A Frequency Tunable Circulator with 70 dB Isolation Using Reflection Coefficient Controller for Arbitrary Load Impedance

Donghyun Lee, Gisung Yang, Jong-Hyuk Park and Byung-Wook Min, *Member, IEEE*

***Abstract*—This paper presents a method to increase the isolation and control the operating frequency of a circulator. The internal signal flow of a circulator is analyzed, and the through-port reflection to cancel out leakage signal is investigated. A reflection coefficient controller(RCC) is designed to ensure that such reflection occurs at the operating frequency. In addition, the operating frequency can be tuned by using two varactor diodes of the RCC for an arbitrary value of the antenna impedance. The experimental results from the proposed method show an isolation of 70 dB and an insertion loss of –1.4 dB at the operating frequency. Moreover, the operating frequency can be changed from 2.2 GHz to 2.8 GHz with high isolation for an arbitrary antenna impedance.**

***Index Terms*—full-duplex radio(FDR), signal cancellation, high isolation circulator, tunable circulator, arbitrary impedance matching, reflection coefficient controller.**

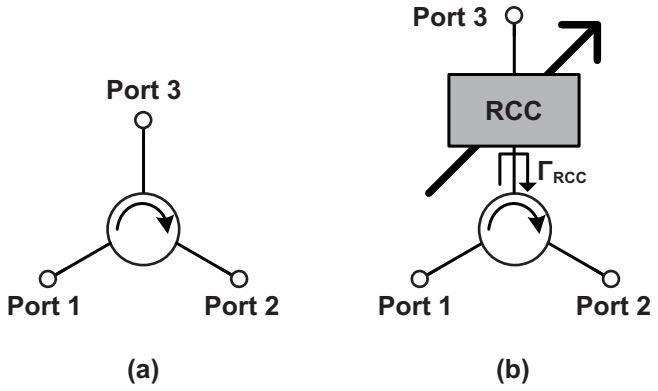

Fig. 1. Circulators for two configurations: (a) without RCC, (b) with RCC.

I. Introduction

IN-band full-duplex radio systems have recently attracted interest for solving radio frequency (RF) congestion. Full-duplex radio (FDR) systems which transmit and receive simultaneously using the same frequency resources, ideally increase the spectral efficiency by a factor of two[1]. However, there is a self interference problem in such systems since the signal radiated from the transmitter interferes with the desired signal received by the antenna where the power of the latter signal is very low compared to that of the former [2]. Thus, high isolation between the transmitter (TX) and receiver (RX) is essential in an FDR system, and this isolation can be achieved by antenna isolation, RF cancellation, and digital cancellation [2-3]. Generally, a ferrite circulator with an isolation level exceeding 30 dB is required for antenna isolation if a common antenna needs to be shared by the TX and RX [4]. However, typical ferrite commercial circulators have an isolation of approximately 20 dB; therefore, circulators with higher isolation are required for an FDR system.

Geometric changes to ferrite circulators have been studied to improve isolation by modification of the crossover structures [5-7]. Although these changes do not increase insertion losses, the isolation is not improved much and is heavily dependent on the impedance of the antenna port. It has been shown that a circulator with a filter can achieve high isolation between TX and RX; however, the structure is primarily a diplexer, so it cannot be used for a full-duplex system[8]. Another method of obtaining high isolation is the signal cancellation method which involves applying a signal with the same magnitude and opposite phase as the leakage signal at the RX port. In [9], the transmit signal was divided into two circulators and the leakage signal from a circulator cancels the other leakage signals. Comparatively high isolation was achieved in [9] using this scheme; however, the insertion loss of the structure was 3 dB owing to the power divider. In [10], a small portion of the transmitted signal is separated using a coupler followed by a PA; then, it is cancelled with the leakage signal at the coupler following LNA, after adjusted by phase shifter and attenuator to duplicate the leakage signal. This method achieves high isolation, but it is also not free from additional insertion losses due to power division and combination. In addition to the ferrite circulator, there are non ferrite circulators that use transistors, which provide high isolation mainly by signal cancellation. However, most of the available non ferrite circulators have poor insertion losses. Amplifiers are generally used to improve upon this disadvantage, but the problem of linearity degradation remains [11-15].

In this paper, a design theory and practical implementation of a tunable high-isolation circulator using a network called the reflection coefficient controller (RCC) are presented. The proposed structure has high isolation and low insertion loss

Manuscript received xxxxxxx. xx, 2020; revised xxxxxxxx; accepted xxxxxx xx, 2020. Date of publication xxxxxx xx, 2020; date of current version xxxxxx xx, 2020.

The authors are with the Department of Electrical and Electronic Engineering, Yonsei University, Seoul 120-749, Korea (e-mail: bmin@yonsei.ac.kr).

Color versions of one or more of the figures in this brief are available online at http://ieeexplore.ieee.org.

Digital object identifier: xxxxxxxxxxxx

characteristics for an arbitrary value of the antenna impedance with the capability to vary operating frequency, where the isolation performance should be best. Further, the power handling capability is measured and discussed. In Section II, the mathematical design of achieving high isolation is shown with respect to the given S-parameters of the ferrite circulator; the detailed procedure to implement the design using RCC is presented in Section III. The measured results are then given in Section IV, and the conclusions are presented in Section V.

II. Design Theory

A. Reflection coefficient control and isolation

In reality, a general circulator shown in Fig. 1(a) is different from the ideal one owing to the imperfect performance of the ferrite and the geometrical structure within the circulator. The S-parameters of the circulator in Fig. 1(a) can be expressed as

$$S = \begin{bmatrix} S_{11} & S_{12} & S_{13} \\ S_{21} & S_{22} & S_{23} \\ S_{31} & S_{32} & S_{33} \end{bmatrix}. \tag{1}$$

None of these terms is either a perfect 0 or 1, which means that the signal does not flow in one direction and it is impossible to achieve perfect matching unlike an ideal circulator because of the process errors involved in the manufacturing of commercial circulators. In addition, even though S_{21} in (1) is 0, when port 3 is used for an antenna whose impedance is not Z_0, the reflected signal is generated from the port and mixed with the existing signal such as the leakage signal, which affects the performance of the circulator.

In this situation, it is not clear whether the mixture of signals has a good effect on the performance of the circulator. For example, if the reflected signal is in phase with the leakage signal and has a lager magnitude, the isolation performance degrades. Conversely, if the reflected signal is out of phase with the leakage signal but has same magnitude, the isolation performance is improved by cancellation of the signal. The isolation performance of the circulator can thus be determined by adding an RCC, as shown in Fig. 1(b). The S-parameters in Fig. 1(b) can be expressed as

$$S' = \begin{bmatrix} S'_{11} & S'_{12} \\ S'_{21} & S'_{22} \end{bmatrix}. \tag{2}$$

The S-parameters of the two-port network in (2) can be analyzed by reducing a three-port network to a two-port network and finding the modified scattering matrix of the three-port network with one of the ports is not match-terminated; this modification is then described by the S-parameters in (1) and Γ_{RCC}, which is the reflection coefficient of the antenna port in Fig. 1(b) [16-17]. The isolation S'_{21} is expressed as

$$S'_{21} = S_{21} + \frac{S_{31} \times S_{23} \times \Gamma_{RCC}}{1 - S_{33} \times \Gamma_{RCC}}. \tag{3}$$

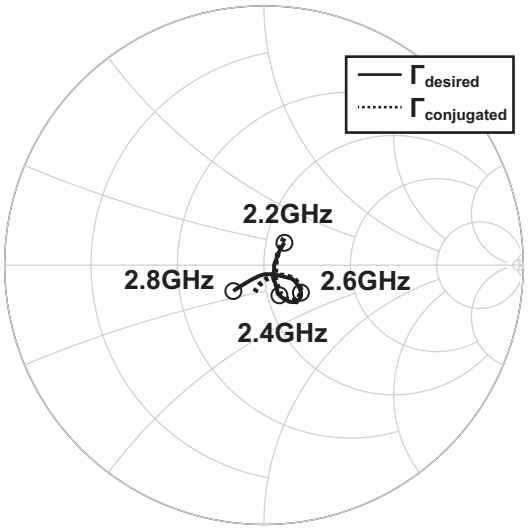

Fig. 2. $\Gamma_{desired}$ and $\Gamma_{conjugated}$ depicted on the Smith chart.

B. Isolation and power transfer efficiency

As shown in Section II-A, the reflected signal at the antenna port affects the S-parameters. In other words, S'_{21} can be adjusted using Γ_{RCC}. To enable the circulator to have high isolation, the value of Γ_{RCC} should be adjusted such that S'_{21} = 0 in (3). Such a desired Γ_{RCC} can be written as

$$\Rightarrow \Gamma_{desired} = \frac{-S_{21}}{S_{31} \times S_{23} - S_{21} \times S_{33}}. \tag{4}$$

In (4), $\Gamma_{desired}$ represents the value of Γ_{RCC} for which S'_{21} is zero. This equation gives an exact formula for Γ_{RCC} to achieve perfect isolation. Thus far, this technique is the only available choice for perfect isolation; however, it is not clear whether this scheme allows good matching, or power delivery. Thus, the transducer power gain should be analyzed. Theoretically, maximum power transfer can be achieved by conjugate matching at the antenna port. The calculated $\Gamma_{desired}$ and $\Gamma_{conjugated}$, which is the reflection coefficient at the antenna port when conjugate matching is performed using the measured S-parameters of a commercial circulator, SKYFR-000742, are shown in Fig. 2.

Fig. 2 shows that $\Gamma_{desired}$ resembles $\Gamma_{conjugated}$, which leads to the expectation that the transducer power gain from port 1 to the antenna and from the antenna to port 2 when Γ_{RCC} = $\Gamma_{desired}$ is almost equal to that of the case when maximum power is transferred. For accurate comparisons, the transducer power gain at the TX port for each case where the RCC is assumed to be lossless is shown in Fig. 3 and that for the RX port is omitted since it is almost similar to that of the TX.

As shown in Fig. 3, the transducer power gain without the RCC is lower than that where Γ_{RCC} = $\Gamma_{desired}$, whereas there is no significant difference between the cases where Γ_{RCC} =

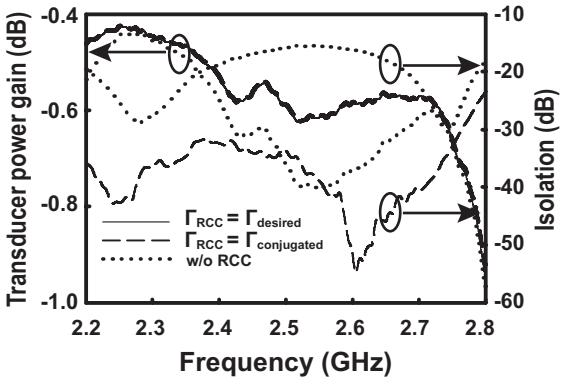

Fig. 3. Calculated transducer power gains and isolations with respect to the TX port for each case based on the measured S-parameters of a commercial circulator, SKYFR-000742. Isolation for the case where Γ_{RCC} = $\Gamma_{desired}$ is not shown as it is infinite.

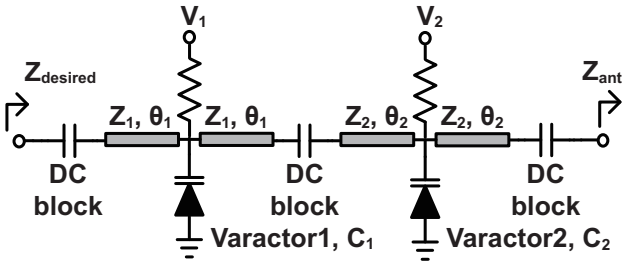

Fig. 4. Schematic of the proposed reflection coefficient controller (RCC).

$\Gamma_{desired}$ and Γ_{RCC} = $\Gamma_{conjugated}$, as expected. Numerically, the difference is less than 0.005 dB from 2.2 GHz to 2.7 GHz and 0.03 dB at 2.8 GHz. This isolation is also shown in Fig. 3. The isolation is relatively good for Γ_{RCC} = $\Gamma_{conjugated}$ but not perfect; conversely, it is infinite for the case where Γ_{RCC} = $\Gamma_{desired}$. Therefore, $\Gamma_{desired}$ would be the best choice since the insertion loss for mismatch is negligible but the isolation is greatly improved. At this point, the question arises whether this 'coincidence', i.e., $\Gamma_{desired} \simeq \Gamma_{conjugated}$, occurs only for the specific circulator, SKYFR-000742, measured in this work. Intuitively, it can be considered that if the signal from port 1 does not reach port 2, it is transmitted to some other point in the network because the RCC is assumed to be a lossless network and hence it is not a coincidence.

III. Design of RCC

To achieve high isolation, a circuit that can transform a specific antenna impedance to $\Gamma_{desired}$ must be designed. If the circuit comprises only one transmission line, then it is impossible to transform a range of impedances to $\Gamma_{desired}$. However, if the circuit consists of stepped transmission lines, then it is possible to transform any impedances to the $\Gamma_{desired}$. Thus, starting from the stepped transmission lines, each transmission line section is implemented via synthetic transmission lines using varactors as tunable factors. This RCC network is shown in Fig. 4.

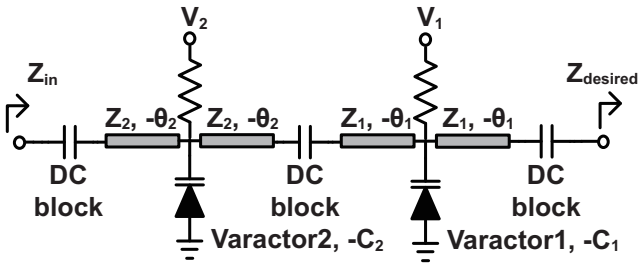

Fig. 5. Schematic of the de-embedding network of the original RCC.

The standard return loss of a conventional antenna is 10 dB, but actually varies from product to product and also depends on the environment in which it is used. Therefore, consideration of the arbitrary antenna impedance is necessary. The recommended operating frequency of the circulator used in this study is 2.5 GHz; hence, the proposed circuit is designed to be tuned from 2.2 to 2.8 GHz, where the insertion loss of the circulator is acceptable, to ensure that any impedance whose return loss is within 10 dB can be transformed to an impedance corresponding to $\Gamma_{desired}$, namely $Z_{desired}$, by adjusting two varactors.

To achieve this, all the design parameters, such as Z_1, θ_1, Z_2, and θ_2, in Fig. 4 should be carefully chosen; however, this may be very difficult owing to the following reasons. Technically, at the frequency of interest, for a given set of design parameters, if an intersection of sets, that represent the areas consisting of reflection coefficients corresponding to the impedances transformed by the RCC starting from all the impedances whose return losses are less than 10 dB, being drawn by sweeping C_1 and C_2 which are the values of the capacitances of the two varactors in the RCC, contains the $\Gamma_{desired}$ of that frequency, then it is done. However, this kind of approach has not only complexity but also does not give the intuition what design parameters should be to do such thing, because the intersection of numerous sets on the Smith chart is hard to consider. Hence, a new design technique based on designing the de-embedding network of the original RCC, instead of the RCC itself, is introduced as follows.

The de-embedding network of the original RCC is the mirror symmetric network, where the electrical lengths of the transmission lines, capacitances, and inductances become negative values as shown in Fig. 5. At the frequency of interest, if the area consisting of the reflection coefficients corresponding to all the Z_{in} in Fig. 6 which are the impedances looking into the de-embedding network of the original RCC named –RCC terminated by $Z_{desired}$ of that frequency, plotted by sweeping $-C_1$ and $-C_2$, which are the values of the negative capacitances of the two varactors in the –RCC, includes 10 dB circle in Smith chart, then it is ensured that the original RCC have a capability to transform all the impedances whose return losses are less than 10 dB to $Z_{desired}$. Unlike the method mentioned in the previous paragraph, as long as the mechanism of impedance transformation on the Smith chart is considered in the opposite manner, for example counter clockwise movement drawn by the transmission line whose

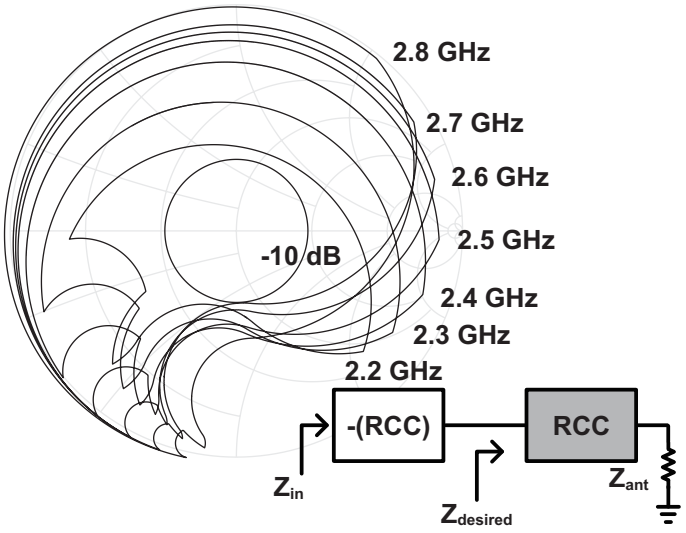

Fig. 6. Traces consisting of Z_{in}s that are transformed by the –RCC, where $-C_1$ and $-C_2$ are swept, starting from $Z_{desired}$ for each frequency on the Smith chart. At a frequency, a closed loop is formed by four traces representing
trace 1 : $-C_{min}$, [$-C_{max}$, $-C_{min}$], trace 2 : [$-C_{max}$, $-C_{min}$], $-C_{min}$,
trace 3 : $-C_{max}$, [$-C_{max}$, $-C_{min}$], trace 4 : [$-C_{max}$, $-C_{min}$], $-C_{max}$.

sign of the electrical length is negative, it is easy to determine the design parameters in the –RCC to do such work since the trace can be considered intuitively that consists of the impedances transformed by the –RCC starting from the single impedance, $Z_{desired}$ of the target frequency.

There is no synthetic closed form solution of the design parameters, Z_1, θ_1, Z_2, and θ_2 over the frequency bandwidth since $Z_{desired}$ of the experimented circulator cannot be expressed as a simple mathematical function of frequency. Furthermore, it is difficult to explain the impedance transformation from any arbitrary impedance by adjusting C_1 and C_2. Therefore, the design process are visualized with the concept of inverse network, –RCC. After choosing a varartor with a high enough self resonance frequency, one can draw a closed loop in Smith chart made by four traces, which are sets of Z_{in}s of –RCC by sweeping $-C_1$ and $-C_2$ independently within the varactor tuning range as in Fig. 6. The parameters, Z_1, θ_1, Z_2, and θ_2 need to be designed iteratively in order that 10-dB arbitrary impedance circle in Smith chart is enclosed by the closed loops of all frequencies of interest. For the given circulator, the design parameters are Z_1 = 75 Ω, θ_1 = 20° @ 2.5 GHz, Z_2 = 48 Ω and θ_1 = 20° @ 2.5 GHz. At the chosen design parameters, the traces are described in the Smith chart in Fig. 6. For each frequency, four vertices on the trace represent the Z_{in}s looking into the –RCC terminated by $Z_{desired}$ when $-C_1$ and $-C_2$ are $-C_{min}$ or $-C_{max}$ and so on. The only remaining part of the design of the RCC is taking mirror symmetry and positive sign to given –RCC.

IV. Implementation and Measured Results of the Proposed Circulator

The proposed circulator is implemented on a Taconic RF-35 substrate, whose thickness is 0.76 mm, using a SKYFR-000742 circulator and two SMV-1405 varactors manufactured by Skyworks with SC-79 package whose parasitic inductance is 0.7 nH and self resonance frequencies are 3.7 GHz and 7.4 GHz for C_{max} and C_{min}, respectively. This setup is shown in Fig. 7. The size of the board is 5 cm × 6 cm, including the SMA connectors. The S-parameters are measured using a Keysight E5071 vector network analyzer and an Anritsu MS2830A spectrum analyzer and Anritsu MG3694C signal generator are used to measure the linearity. The tuning range of voltages used for the varactor is 0–30 V, and the required voltage for high isolation depends on the target frequency and load impedance.

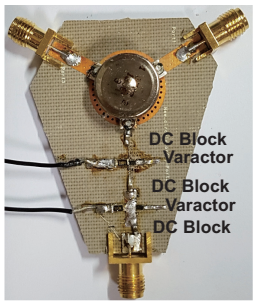

Fig. 7. Photograph of the proposed high isolation circulator with RCC.

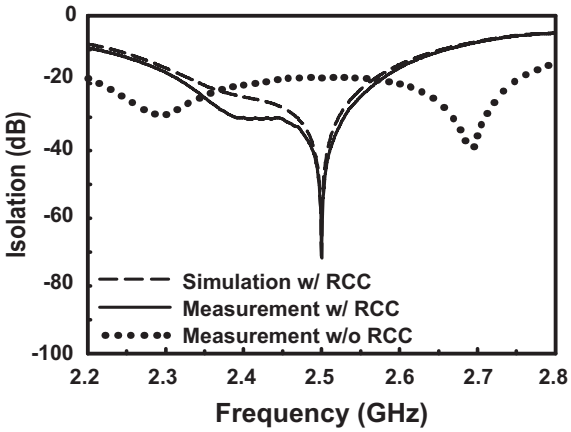

Fig. 8. Simulated and measured isolations for each case tuned at 2.5 GHz when the port for an antenna is terminated by a 50 Ω resistor.

A. S-parameter measurement

To demonstrate the performance of the proposed circulator, the case where the port for an antenna is terminated by a 50 Ω resistor is shown first; then, a commercial monopole antenna is used to verify that the RCC can be applied for arbitrary load impedances as well as the 50 Ω resistor. The results for the former case with and without the RCC, which is tuned at 2.5 GHz, is shown in Fig. 8. The dashed line shows the simulated isolation of the proposed circulator with the RCC, and the solid and dotted lines show the measured isolations of the commercial circulator with the RCC and that without the RCC, respectively. The proposed circulator has a 50 dB higher isolation performance than the commercial circulator. The other characteristics are as follows.

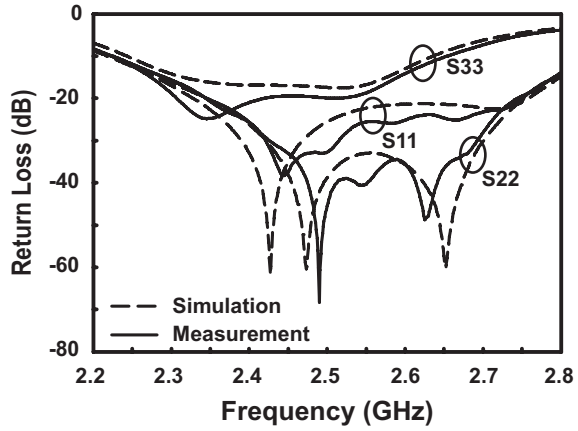

Fig. 9. Simulated and measured return losses tuned at 2.5 GHz when the port for an antenna is terminated by a 50 Ω resistor.

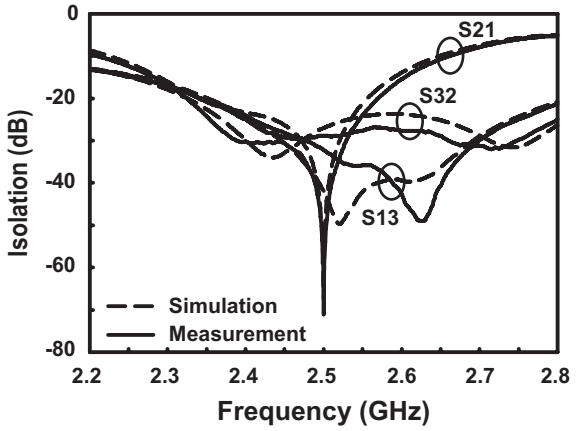

Fig. 11. Simulated and measured isolations of S_{21}, S_{32}, and S_{13} with the RCC tuned to minimize S_{21} at 2.5 GHz.

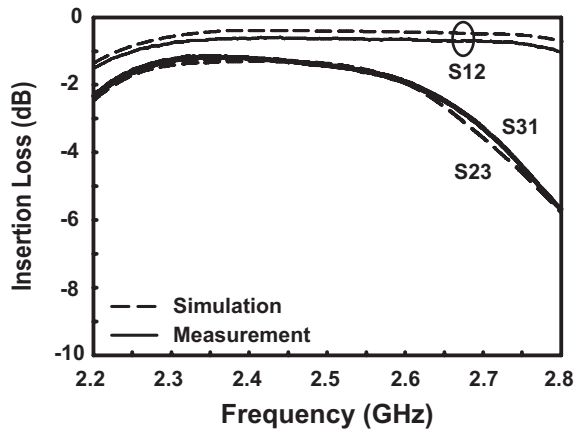

Fig. 10. Simulated and measured insertion losses of the proposed circulator tuned at 2.5 GHz.

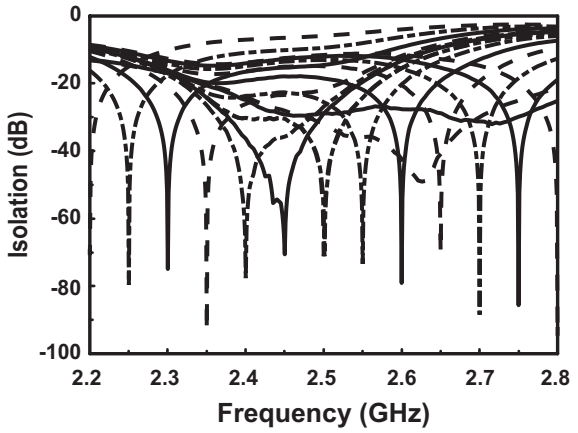

Fig. 12. Measured isolations with the RCC tuned to individual frequencies when the port for an antenna is terminated by 50 Ω resistor. The varactor states for tuning frequencies are summarized in Table I/II.

The measured and simulated results for the return losses are shown in Fig. 9 and that for the insertion losses are shown in Fig. 10, where the dashed and solid lines represent the simulated and measured results, respectively. The return loss is below –20 dB at 2.5 GHz, and the insertion loss for S_{12} is about –0.6 dB, and the insertion losses for S_{31} and S_{23} are about –1.4 dB each, mainly caused by the series resistances of the varactors in the RCC.

The other isolation cases that are not depicted in Fig. 8 are shown in Fig. 11. The isolation for S_{21} is 70 dB and that for S_{13} and S_{32} are below –20 dB. The isolations for S_{13} and S_{32} with the RCC maintain the isolation of the circulator without the RCC because the magnitude of the adjusted reflection coefficient for high isolation is small for S_{21}; thus, S_{13} and S_{32} are not affected much. To summarize, the proposed circulator has a loss of 0.8 dB owing to the RCC and an isolation of 70 dB, while maintaining the return losses, other insertion losses, and isolation characteristics of the circulator used in the design. Fig. 12 shows the isolations for the cases where the bias voltages applied to each of the varactors in the RCC are optimized for each frequency to obtain high isolation with 50 Ω termination, and most of these are observed to be over 70 dB.

Finally, a commercially available monopole antenna, whose return loss is as shown in Fig. 14, is used to verify the ability of the RCC to obtain high isolation with arbitrary load impedances instead of 50 Ω, as depicted in Fig. 13. The measured isolations corresponding to Fig. 12 in this case are shown in Fig. 15, and the return losses are omitted for

TABLE I
TUNING FREQUENCIES AND VARACTOR STATES OF THE RCC FOR 50 Ω TERMINATION

f_0 (GHz)	C_1 (pF)	C_2 (pF)	V_1 (V)	V_2 (V)
2.2	3.04	2.78	0.46	0.66
2.3	2.9	2.74	0.64	0.78
2.4	2.58	2.66	1.05	0.96
2.5	2.26	2.45	1.66	1.34
2.6	2.05	2.13	2.28	2.06
2.7	2.02	1.81	2.52	3.25
2.8	2.12	1.85	2.43	3.28

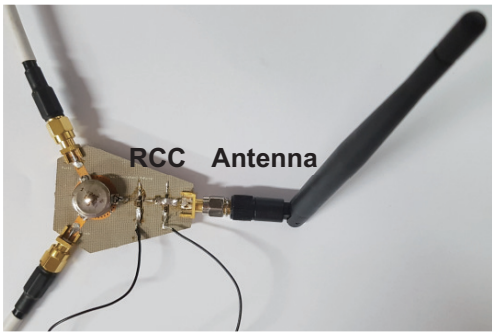

Fig. 13. Photograph of the proposed circulator with the monopole antenna.

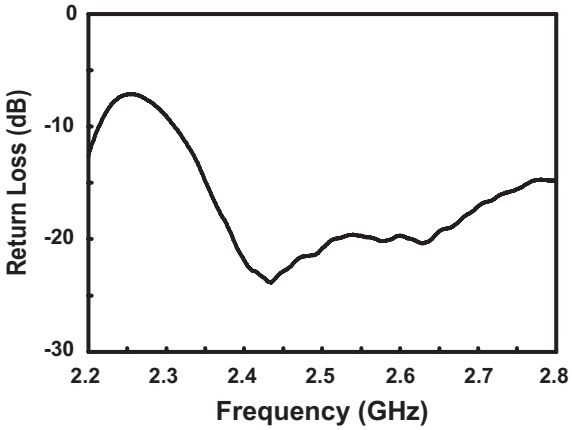

Fig. 14. Measured return loss of the monopole antenna.

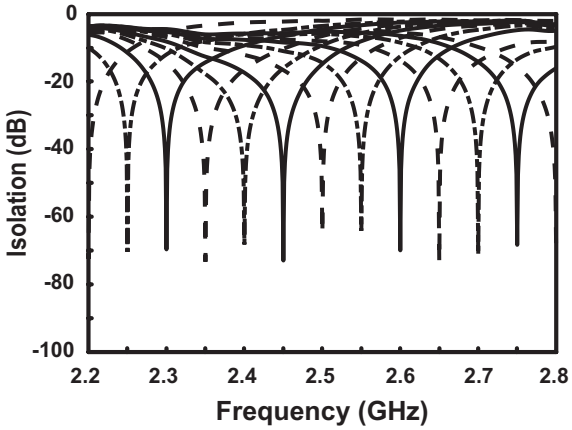

Fig. 15. Measured isolations with the RCC tuned to each frequency when the port for an antenna is terminated with a monopole antenna. The varactor states for tuning frequencies are summarized in Table I/II.

simplicity since they do not differ from those of 50 Ω case.

B. Power handling capability

Since the proposed circulator is based on a commercial passive circulator whose linearity is generally high, the power handling capability is dominated by the linearity of the varactors in the RCC. As the input power increases, thereby the voltage swings of the varactors increase, affecting the isolation and insertion loss of the proposed circulator. Fig. 16 shows

TABLE II
TUNING FREQUENCIES AND VARACTOR STATES OF THE RCC FOR A MONOPOLE ANTENNA

f_0 (GHz)	C_1 (pF)	C_2 (pF)	V_1 (V)	V_2 (V)
2.2	2.81	2.23	0.64	1.34
2.3	2.85	3.4	0.69	0.32
2.4	2.65	2.78	0.97	0.84
2.5	2.26	2.58	1.65	1.16
2.6	2.22	2.16	1.88	2
2.7	2.22	1.64	2.03	4.1
2.8	2.15	1.55	2.34	4.91

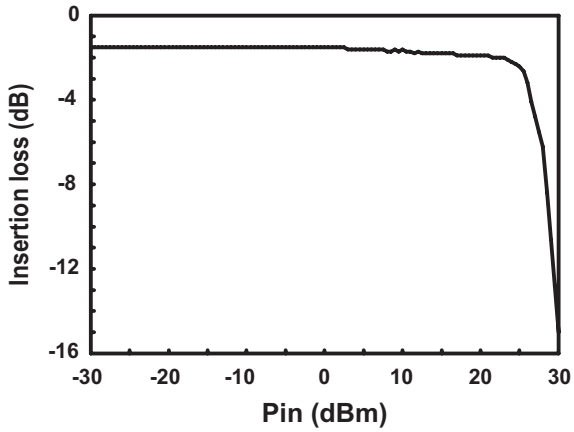

Fig. 16. Measured insertion loss (TX to antenna) of the proposed circulator with RCC versus input power at 2.5 GHz with 50 Ω termination.

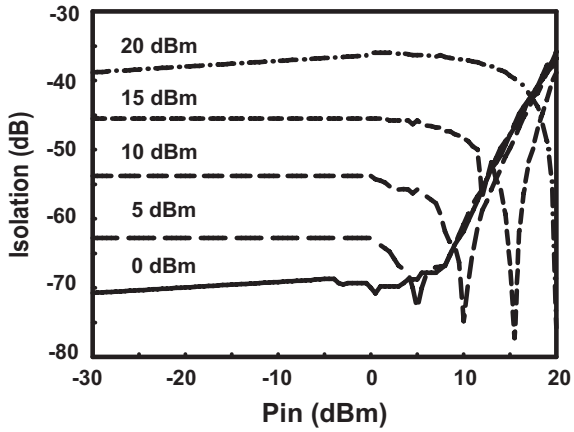

Fig. 17. Measured isolation of the proposed circulator with RCC versus input power at 2.5 GHz with 50 Ω termination. Varactors of RCC are tuned at the input power level indicated.

the measured insertion loss from TX port to antenna port versus input power, and the 1-dB power compression point is 25 dBm. The varactors of RCC are tuned for the highest isolation at 2.5 GHz with 50 Ω termination at the input power level of 0 dBm. Fig. 17 shows the measured isolation between TX and RX ports versus input power, and the varactors of RCC are tuned at various power level of 0-20 dBm. The isolation is maximized at the input power when the varactors

TABLE III
PERFORMANCE COMPARISON WITH OTHER REFERENCES

	This work	[9]	[18]	[20]	[19]
Frequency tunability (GHz)	Yes (2.2∼2.8)	No	Yes (1.8∼2.8)	Yes (67∼85)	No
Center frequency (GHz)	2.45	1.9	2.4	78	0.93
$>$ 40 dB isolation fractional bandwidth (%)	2.04	1.05	0.42	3.84	4.3
Return loss (dB)	-20	N/A	-20	-10	-10
S_{31}	-1.4	-8	-2.2	-9	-1
S_{23}	-1.4	-8.5	-3.2	-3	-1
S_{21}	-72	-66	-65	-55	-60

are tuned. For the small signal power of 0 dBm, the 1-dB power expansion point is 9 dBm which is lower than the 1-dB power compression point of insertion loss since the power level of leakage signal is much lower than the power level of transmitting signal especially with a high isolation. It is possible to optimize the bias voltages of the varactors in the RCC for a specific input power level as shown in Fig. 17, but the optimization is less effective for the modulated signal with a high peak to average power ratio. This is expected rather naturally since any technique for the RCC to have high linearity such as anti-series topology for utilizing varactors is not used; these cases are relegated to future work.

C. Comparison of performance with other references

Comparison of performance with other references is shown in Table III. As mentioned in the introduction, [9] and [18] shows high insertion loss owing to the coupler functioning as power divider and combiner. Although there is no coupler in [20] directly, the mechanism to achieve high isolation is basically same as [9], which also shows high insertion loss and low SNR. A direct matching network is added between a circulator and a port for an antenna in [19], which makes insertion loss low, but unlike [19], the RCC has frequency tunability and strict theoretical requirement for the RCC is covered in this work.

V. CONCLUSION

A frequency tunable high isolation circulator with 70 dB isolation is presented in this paper. The desired reflection coefficient for high isolation, looking into the antenna port with respect to the circulator, is derived and observed to not differ much from the conjugated reflection coefficient for maximum power transfer; this leads to the observation that the loss of transducer power gain in the former case is negligible compared to that in the latter case. A circuit referred to as the reflection coefficient controller (RCC) is thus designed and attached between the load and circulator to adjust the load impedance to the desired impedance corresponding to the desired reflection coefficient. Before implementing the RCC, its de-embedding network is designed in advance, which is a versatile technique to ensure that the given circuit can transform any load impedance to the desired impedance corresponding to the desired reflection coefficient at the frequency of interest. The measured results show that the proposed circulator achieves a high isolation of 70 dB for the load as commercially available monopole antenna as well as a 50 Ω termination, and the operating frequency for the isolation maximization should be maximized can be varied in the range of 2.2–2.8 GHz by tuning the varactors in the RCC, while maintaining a low insertion loss of 1.4 dB. The proposed circulator is suitable for communication systems such as in-band full duplex radio.

REFERENCES

[1] A. Gupta and R. K. Jha, "A survey of 5G network: Architecture and emerging technologies," *IEEE Access.*, vol. 3, pp. 1206-1232, 2015.

[2] D. Bharadia, E. McMilin and S. Katt, "Full duplex radios," *ACM SIGCOMM Comput. Commun. Rev.*, vol. 43, no. 4, pp. 375-386, 2013.

[3] A. Sabharwal, P. Schniter, D. Guo, D. W. Bliss, S. Rangarajan, and R. Wichman, "In-band full-duplex wireless: Challenges and opportunities," *IEEE J. Sel. Areas Commun.*, vol. 32, no. 9, pp. 1637-1652, Sep. 2014.

[4] N. Reiskarimian, J. Zhou, H. Krishnaswamy, "A CMOS passive LPTV nonmagnetic circulator and its application in a full-duplex receiver", IEEE J. Solid-State Circuits, vol. 52, no. 5, pp. 1358-1372, May 2017.

[5] L. K. Anderson, "An analysis of broadband circulators with external tuning elements," *IEEE Trans. Microwave. Theory Techn.*, vol. 15, no. 1, pp. 42-47, 1967.

[6] Y. Konishi, "New theoretical concept for wide band gyromagnetic devices," *IEEE Trans. Magnetics.*, vol. 8, no. 3, pp. 505-508, 1972.

[7] H. Dong, J. R. Smith and J. L. Young, "A wide-band, high isolation UHF lumped element ferrite circulator," *IEEE Microw. Wireless Compon. Lett.*, vol. 23, no. 6, pp. 294-296, 2013.

[8] Kusumoto, Yusuke, et al., "A novel 4-port lumped element circulator for high-isolation duplex architecture," in Proc. *IEEE MTT-S Int. Microw. Symp.*, pp. 1-4, May. 17-22, 2015.

[9] Po-Wen Chen, Mu-Tsung Lai, Hen-Wai Tsao and Jing-Shown Wu, "A high isolation quasi-circulator with self-adjusting technique," in Proc. *Asia-Pacific Microwave Conference (APMC)*, pp. 268-270, Nov. 4-7, 2015

[10] Kolodziej, K. E., J. P. Doane, and B. T. Perry. "Single antenna in-band full-duplex isolation-improvement techniques." in Proc. *Antennas and Propagation (APSURSI), 2016 IEEE International Symposium on*, pp. 1661-1662, June. 26, 2016.

[11] H.-S. Wu, C.-W. Wang, C.-K. Tzuang, "CMOS active quasi-circulator with dual transmission gains incorporating feedforward technique at K-band", *IEEE Trans. Microw. Theory Techn.*, vol. 58, no. 8, pp. 2084-2091, 2010.

[12] He, S., N. Akel, and C. E. Saavedra. "Active quasi-circulator with high port-to-port isolation and small area." *Electronics letters*, 48.14 (2012): 848-850.

[13] D. J. Huang, J. L. Kuo, H. Wang, "A 24-GHz low power and high isolation active quasi-circulator." in Proc. *IEEE MTT-S Int. Microw. Symp. Dig.*, pp. 1-3, June. 17-22, 2012.

[14] Hsieh, Jian-Yu, Tao Wang, and Shey-Shi Lu, "A 1.5-mW, 2.4 GHz quasi-circulator with high transmitter-to-receiver isolation in CMOS technology," *IEEE Microw. Wireless Compon. Lett.*, vol. 25, no. 12, pp. 872-874, 2014.

[15] M. Porranzl, C. Wagner, H. Jaeger, and A. Stelzer, "A New Active Quasi Circulator Structure with High Isolation for 77-GHz Automotive FMCW Radar Systems in SiGe Technology," in Proc. *Compound Semiconductor Integrated Circuit Symposium (CSICS*), pp. 1-4, Oct. 11-14, 2015

[16] R. K. Mongia, I. J. Bahl, P. Bhartia, and J. Hong, *RF and Microwave Coupled-Line Circuits.* Norwood, MA: Artech House, pp. 48-49, 1999.

[17] J. L. Young, R. S. Adams, B. O'Neil, and C. M. Johnson, "Bandwidth Optimization of an Integrated Microstrip Circulator and Antenna Assembly: Part 1," *IEEE Antennas Propag. Mag.*, vol. 48, no. 6, pp. 47-56, 2006.

[18] T. Pochiraju and V. Fusco, "Reflection/transmission tuner analysis and applications," *IET Microwave. Antennas Propag.*, vol. 4, pp. 1387- 1396, Sep. 2010.

[19] C. F. Campbell, J. A. Lovseth, S. Warren, A. Weeks, P. B. Schmid, "A BST Varactor Based Circulator Self Interference Canceller for Full Duplex Transmit Receive Systems" *IEEE MTT-S Int.Microw. Symp.*, pp. 1-4, Aug. 4-6 2020.

[20] Porranzl, Matthias, et al. "An active quasi-circulator with controllable leakage canceler and passive TX path for 77-GHz automotive FMCW radar systems in SiGe technology." *Microwave Conference (APMC)*, 2015 Asia-Pacific. Vol. 1. IEEE, 2015.

Donghyun Lee was born in Suwon, Korea, in 1988. He received the B.S. degree in electrical and electronic engineering from Yonsei University, Seoul, Korea, in 2014. He is currently pursuing the Ph.D. degree in electrical and electronic engineering at Yonsei University, Seoul, Korea.

Gisung Yang was born in Gwangmyeong, Korea. He received the B.S. degree in electrical and electronic engineering from Yonsei University, Seoul, South Korea, in 2020, where he is currently pursuing the Ph.D. degree in electrical and electronic engineering. His current topics of study include optimization techniques for tuning RF canceller in in-band full duplex RF front-end by a machine learning.

Jong-Hyuk Park was born in Seoul, Korea, in 1991. He received the B.S. degree from University of Seoul, Seoul, Korea, in 2016, and a M.S degree from Yonsei University, Seoul, Korea in 2018. His research interests include tunable matching networks, adaptive impedance matching networks and circulators for in-band full duplex and radar systems. He joined the Hyundai Mobis Company, Gyeonggi-Do, Korea, in 2018, where he is currently involved with the RF Communication cell.

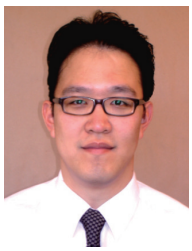

Byung-Wook Min was born in Seoul, Korea. He received his B.S. degree from Seoul University, Seoul, Korea, in 2002, and his M.S. and Ph.D degrees in electrical engineering and computer science from the University of Michigan at Ann Arbor in 2004 and 2007, respectively. During 2006-2007, he was a visiting scholar with the University of California at San Diego, La Jolla.

He is currently an Associate Professor with the Department of Electrical and Electronic Engineering, Yonsei University, Seoul, Korea. During 2008-2010, he was a senior engineer at Qualcomm Inc., Santa Clara, CA and Austin, TX. His research interests include Si/SiGe RFIC and communication systems for microwave and millimeter-wave applications.